

Searching for the Lightest Neutralino at Fixed Target Experiments

L. Borissov, J. M. Conrad, M. Shaevitz
Columbia University, New York, NY, 10027
 (December 2, 2024)

Most ongoing supersymmetry searches have concentrated on the high-energy frontier. High-intensity fixed target beam-lines, however, offer an opportunity to search for supersymmetric particles with long lifetimes and low cross-sections in regions complementary to the ones accessible to collider experiments. In this paper, we consider R -parity violating supersymmetry searches for the lightest neutralino and use the NuTeV experiment as an example for the experimental sensitivity which can be achieved.

I. MOTIVATION

A review of supersymmetric models can be found in [1]. We consider models where the lightest neutralino ($\tilde{\chi}_1^0$) is the Lightest Supersymmetric Particle (LSP). If the LSP is allowed to decay, R -parity violation (\mathcal{R}_p) is required via the superpotential:

$$W_{\mathcal{R}_p} = \lambda_{ijk} L_i L_j \bar{E}_k + \lambda'_{ijk} L_i Q_j \bar{D}_k + \lambda''_{ijk} \bar{U}_i \bar{D}_j \bar{D}_k \quad (1)$$

where i, j and k are generation indices, L and Q are the lepton and quark $SU(2)$ superfield doublets, E, U , and D are the lepton and quark singlets and λ_{ijk} , λ'_{ijk} , and λ''_{ijk} are Yukawa-type couplings between the fields. This model is specified by the squark and slepton masses; mass terms for the gauginos at the electroweak scale (M_1, M_2 and M_3), the ratio of vacuum expectation values of the two neutral Higgses ($\tan\beta$); a mass term mixing the two Higgs doublets (μ) and the values of the λ -couplings.

In the Minimal Supersymmetric Standard Model (MSSM), unification is imposed at the GUT-scale, which leads to the relation:

$$M_1 = \frac{5}{3} \tan^2 \theta_W M_2 \approx 0.5 M_2 \quad (2)$$

where θ_W is the weak mixing angle at the electroweak scale. Assuming Eq. (2), current LEP data give $m_{\tilde{\chi}_1^0} > 32.3$ GeV [9,22]. In the \mathcal{R}_p scenario, collider experiments require the $\tilde{\chi}_1^0$ to decay inside the detector. This leads to very low sensitivity for a long lifetime low mass $\tilde{\chi}_1^0$ [9]. Moreover, if the GUT-scale unification requirement (2) is not assumed, such neutralinos can be produced in observable quantities in lifetime regions inaccessible to collider experiments. Coverage in these regions can be achieved by a detector far from the collision vertex, provided there is enough luminosity and cross-section for neutralino production.

In the following analysis, we present an example of the experimental sensitivity for \mathcal{R}_p SUSY with lepton number violation ($\lambda_{ijk} > 0$) of a high-intensity fixed target experiment. We are interested in very low mass $\tilde{\chi}_1^0$, so we do not require the relation given in Eq. (2), leaving M_1 and M_2 to be free parameters. However, bounds from the invisible decay of the Z^0 necessitate that M_1 is very small compared to M_2 , so that the $\tilde{\chi}_1^0$ is mostly bino and only its Higgsino admixture couples to the Z^0 [8,12]. Thus we work in the framework of phenomenologically motivated \mathcal{R}_p unconstrained MSSM (uMSSM). However our model is very close to the MSSM except for GUT-scale unification and R -parity conservation.

II. AN EXAMPLE: NUTEV

The NuTeV experiment (E815) [17–19] took data during the 1996-1997 fixed target run at Fermilab. NuTeV was designed to perform precision measurements of Standard Model parameters through deep inelastic neutrino-nucleon scattering. These measurements provide competitive and in many cases unique tests of the present-day understanding of the Standard Model, complementary to direct measurements from collider experiments.

During the run, 800 GeV protons from the Tevatron are incident upon a 20.5 cm BeO target at a 7.8 mrad angle. A total of 2.86×10^{18} protons on target were recorded during the live time of the detector. The protons interact and produce a secondary beam of pions, kaons and other hadrons. A system of quadrupole magnets – the Sign-Selected Quadrupole Train (SSQT) picks out secondaries of the correct sign and dumps wrong sign particles. After focusing, the pions and kaons enter a 541 m decay pipe, where they decay in flight with dominant modes $\pi \rightarrow \nu_\mu \mu$, $K \rightarrow \nu_\mu \mu$ and $K \rightarrow \pi^0 \nu_\mu \mu$. Approximately 3% of the mesons decay in the pipe, the rest are dumped in 6 m of aluminum and steel. The muons range out in 241 m of steel shielding and 582 m of earth berm. The resulting beam is a nearly pure neutrino beam with less than 0.2% contamination; it exhibits a dichromatic spectrum corresponding to the superposition of π and K decay distributions.

The NuTeV detector is situated 1.5 km downstream from the target. The calorimeter consists of 168 steel plates ($3 \text{ m} \times 3 \text{ m} \times 5.1 \text{ cm}$), 84 liquid scintillation counters (every 10.2 cm of steel) and 42 drift chambers (every 20.4 cm of steel) followed by a 15 kG toroidal spectrometer. Upstream of the calorimeter is a 35 m decay re-

gion consisting of three large helium bags and six drift chambers (Fig. 1). The decay channel is shielded by an upstream veto wall.

A. Production and decay

At the NuTeV target, $\tilde{\chi}_1^0$'s can be pair-produced in the s -channel via a Z , or in the t -channel through an exchange of a squark (Fig. 2). If the squark mass is sufficiently small, production can be enhanced. For our estimates, however, we have chosen to work with sfermion masses of the order of 800 GeV, conservatively above present experimental bounds [8]. Thus the only relevant production parameters are M_1, M_2, μ , and $\tan\beta$. Production is insensitive to M_3 , which is responsible for the gluino mass.

NuTeV uses a high intensity proton beam, but its center-of-mass energy ($\sqrt{s} \approx 39$ GeV) is low compared to collider experiments. This, however, simplifies the search, since the only relevant mode at this energy is neutralino pair production.

In \tilde{R}_p MSSM, the $\tilde{\chi}_1^0$ decays leptonically according to the diagrams shown in Fig. 3. It is often assumed that only one of the LLE operators in Eq. (1) has a sizeable λ_{ijk} coupling, in order to explain the smallness of L -violating terms in the renormalizable Lagrangian required by present limits [11]. This is also the case of greatest experimental interest. For example, if λ_{122} is dominant, the $\tilde{\chi}_1^0$ decays into $\nu_e \mu^+ \mu^-$ and $\nu_e e^\pm \mu^\mp$ with branching ratios of approximately 50% in each of the two channels [9]. The final state of two leptons and missing energy can be easily detected by an experiment such as NuTeV. The other extreme case, λ_{133} dominant, leads to decays mainly into taus and electrons. The efficiencies for the other λ_{ijk} couplings lie between these two cases.

The partial width for the $\tilde{\chi}_1^0$ decaying into $\nu l l'$ is of the typical form for a fermion three-body decay [11]:

$$\Gamma_{\tilde{\chi}_1^0} = K^2 \frac{G_F^2 m_{\tilde{\chi}_1^0}^5}{192 \pi^3} \quad (3)$$

where K is an effective four-fermion coupling in $\tilde{\chi}_1^0$ decays (Fig. 3) proportional to the $\tilde{\chi}_1^0 f \tilde{f}$ coupling and the \tilde{R}_p coupling λ_{ijk} . For a large region of SUSY parameter space

$$K \sim 0.1 \left(\frac{100 \text{ GeV}}{m_{\tilde{f}}} \right)^2 \lambda_{ijk} \quad (4)$$

where $m_{\tilde{f}}$ is the mass of the virtual selectron or sneutrino exchanged [12].

Upper bounds on λ_{ijk} can be found in Refs. [11,13]. The ones pertinent to our case of study are:

$$\lambda_{122} < 0.049 \times \frac{m_{\tilde{e}_R}}{100 \text{ GeV}} \quad (5)$$

$$\lambda_{133} < 0.006 \times \sqrt{\frac{m_{\tilde{\tau}}}{100 \text{ GeV}}} \quad (6)$$

which come from current universality requirements and limits on ν_e mass [13].

Eq. (4) can be rewritten in terms of the average decay length in the lab frame:

$$l(\text{cm}) = 0.3(\beta\gamma) \left(\frac{m_{\tilde{f}}}{100 \text{ GeV}/c^2} \right)^4 \left(\frac{1 \text{ GeV}/c^2}{m_{\tilde{\chi}_1^0}} \right)^5 \frac{1}{\lambda^2} \quad (7)$$

B. Predictions for the NuTeV experiment

The expected number of $\tilde{\chi}_1^0$ decays detectable by NuTeV is the product of the number $\tilde{\chi}_1^0$'s produced at the target passing through the detector and the probability that any of them actually decays in the He decay region (Fig. 1).

$$N_{evt} = \left(N_p d N_A \rho_{BeO} \frac{d\sigma}{d\Omega} d\Omega \right) \times \frac{(1 - e^{-\Delta z/l})}{e^{z/l}} \quad (8)$$

where $N_p = 2.8 \times 10^{18}$ is the the number of protons on target, d is the length of the BeO target, $\rho_{BeO} = 2.7 \text{ g/cm}^3$ is the target mass density, N_A is Avogadro's number; $d\sigma/d\Omega$ is the differential production cross-section in the center-of-mass reference frame of the pair-production, $d\Omega \approx 1.68 \times 10^{-3} \text{ rad}$ is the solid angle subtended by the detector in that reference frame; z is the distance between the target and the decay region, Δz is the length of the decay region and $l = \gamma c \tau$ is the $\tilde{\chi}_1^0$ decay length in the lab frame. For the NuTeV specifications, equation (8) gives:

$$N_{evt} \approx \left(2.4 \times 10^{14} \text{ mb}^{-1} \frac{d\sigma}{d\Omega} \right) \times \frac{1 - e^{-\frac{3.5 \times 10^3 \text{ cm}}{l}}}{e^{\frac{1.5 \times 10^5 \text{ cm}}{l}}} \quad (9)$$

From Eq. (9), we make a contour plot of the expected number of observable $\tilde{\chi}_1^0$ decays versus $d\sigma/d\Omega$ and l as shown in Fig. 4. Since the expected signal is small, we use a Feldman and Cousins approach for the analysis [20]. The confidence level contours obtained are shown on Fig. 4. We continue to work with the decay length in the lab frame, since it conveniently folds the uncertainty in λ_{ijk} , the sfermion mass and the $\tilde{\chi}_1^0$ mass, which are not very rigidly constrained by present SUSY searches. Moreover, the range of l can be estimated by direct experimental observation. If such an experiment sees a non-zero signal, phenomenological information about the $\tilde{\chi}_1^0$ mass can be incorporated to constrain the remaining SUSY parameters.

As an example for the experimental sensitivity, we consider the hypothetical case of 0 events, i.e. very low signal. We assume 0 background, which is consistent with background estimates for the NuTeV experiment [21].

Using a Monte Carlo event generator [14,15], we perform a scan of uMSSM parameter space for $M_1 = 1, 10, 100 \text{ GeV}/c^2$, $M_2 = 0, \dots, 400 \text{ GeV}/c^2$, $\mu = -200, \dots, 200 \text{ GeV}/c^2$ and $\tan\beta = 1.5, \dots, 40$. We set $m_{\tilde{f}} \approx 800 \text{ GeV}/c^2$ and $M_3 = 1 \text{ TeV}$. We found no strong dependence on M_1 and $m_{\tilde{f}}$, as long as $M_1 \ll M_2$ so that $\tilde{\chi}_1^0$ is mostly bino. We consider $M_1 = 1 \text{ GeV}/c^2$ as representative for the case accessible to NuTeV and similar fixed target experiments and present results for three typical decay lengths, $l = 1.5 \times 10^5, 10 \times 10^5, 15 \times 10^5 \text{ cm}$, for which NuTeV has sensitivity to the discussed signatures. The results for small and large $\tan\beta$ are shown on Fig. 5 and Fig. 6 respectively. These plots should be compared with similar limits obtained by the LEP experiments [9] with the assumption that $\tilde{\chi}_1^0$ decays inside the LEP detectors.

III. CONCLUSIONS

The work presented here is an attempt to motivate R_p searches at fixed target experiments, since collider experiments run into sensitivity problems at low energy [8,9]. We argue that NuTeV and similar fixed target experiments, such as KTeV, may be in a unique position to complement collider searches. At the time of the submission of this publication, NuTeV has announced a non-zero signal in one of the modes discussed above. Preliminary studies under way indicate that the MINOS/NuMI experiment may be sensitive to the NuTeV signal.

IV. ACKNOWLEDGEMENTS

We would like to thank to C. Quigg, J. Lykken, M. Carena, V. Barger, P. Nienaber and the NuTeV collaboration. This research was supported by the U.S. Department of Energy and the National Science Foundation.

- [10] B. Allanach *et al.*, hep-ph/9906224.
- [11] V. Barger, G.F. Giudice and T. Han, Phys. Rev. **D40**, 2987 (1989).
- [12] H.E. Haber and G.L. Kane, Phys. Rept. **117**, 75 (1985).
- [13] B.C. Allanach *et al.*, hep-ph/9906209.
- [14] S. Mrenna, Comput. Phys. Commun. **101**, 232 (1997) hep-ph/9609360.
- [15] T. Sjostrand, hep-ph/9508391.
- [16] D. Choudhury, H. Dreiner, P. Richardson and S. Sarkar, hep-ph/9911365.
- [17] D. A. Harris *et al.* [Nutev Collaboration], hep-ex/9908056.
- [18] J. Conrad *et al.*, Rev. Mod. Phys. **70**, 4 (1998).
- [19] J. Yu *et al.* [Nutev Collaboration], FERMILAB-TN-2040.
- [20] G. J. Feldman and R. D. Cousins, Phys. Rev. **D57**, 3873 (1998)
- [21] J. A. Formaggio *et al.*, hep-ex/9912062.
- [22] ALEPH collaboration, preprint ALEPH 99-011, CONF 99-006

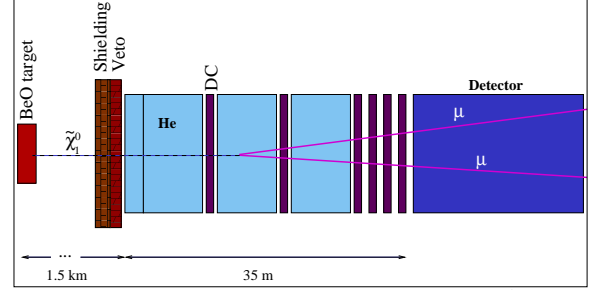


FIG. 1. The NuTeV decay channel. A possible $\tilde{\chi}_1^0 \rightarrow \nu_e \mu^+ \mu^-$ decay is shown as seen by the detector.



FIG. 2. Neutralino pair production mechanisms.

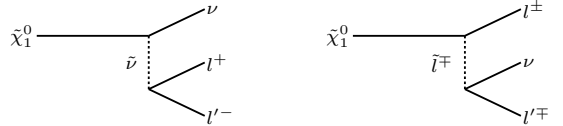


FIG. 3. $R_p \tilde{\chi}_1^0$ decay mechanisms.

-
- [1] S.P. Martin, hep-ph/9709356.
 - [2] V. Barger *et al.*, Phys. Rev. **D50**, 4299 (1994) hep-ph/9405245.
 - [3] H. Dreiner, Pramana **51**, 123 (1998).
 - [4] R.N. Mohapatra, *Maryland Univ. College Park - 86-185 (86,REC.AUG.) 17p*.
 - [5] S. Dimopoulos and L.J. Hall, Phys. Lett. **196B**, 135 (1987).
 - [6] W. Fischler *et al.*, Phys. Lett. **B258**, 45 (1991).
 - [7] L.E. Ibanez and G.G. Ross, Nucl. Phys. **B368**, 3 (1992).
 - [8] C. Caso *et al.*, Eur. Phys. J. **C3**, 1 (1998) Sect. 12.
 - [9] P. Abreu *et al.* [DELPHI Collaboration], CERN-EP-99-049.

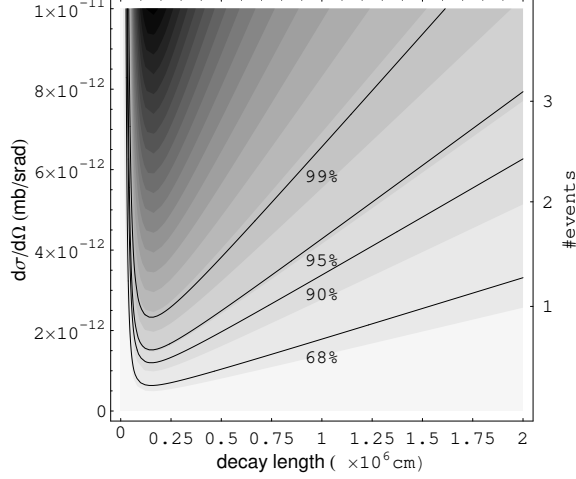


FIG. 4. Contour plots of $\tilde{\chi}_1^0$ pair-production differential cross-section seen by the NuTeV detector versus $\tilde{\chi}_1^0$ decay length in the lab frame. The shaded contours represent the number of $\tilde{\chi}_1^0$ decays occurring inside the detector assuming perfect detector efficiency. The four confidence level contours represent exclusion regions (above the contours) following a Feldman and Cousins approach for 0 signal events and 0 background [20].

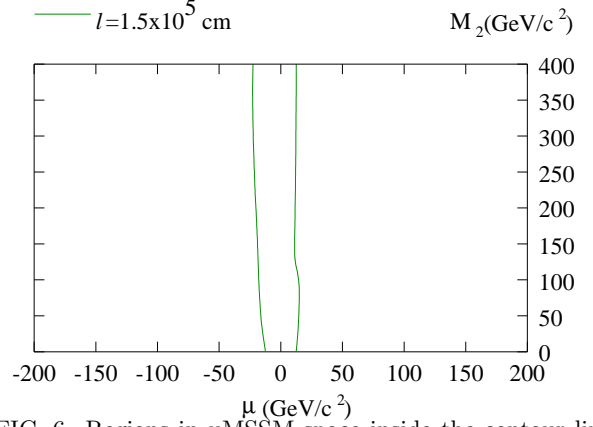


FIG. 6. Regions in uMSSM space inside the contour lines are excluded for large $\tan\beta = 30$ at $M_1 = 1 \text{ GeV}/c^2$. The NuTeV detector has no sensitivity for decay lengths much larger than $1.5 \times 10^6 \text{ cm}$ for large $\tan\beta$.

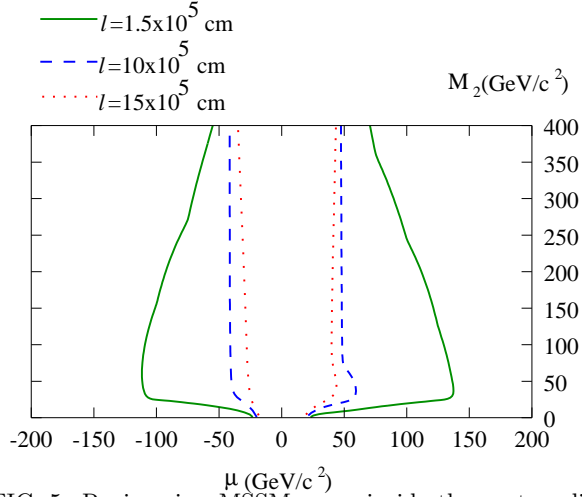


FIG. 5. Regions in uMSSM space inside the contour lines are excluded for small $\tan\beta = 1.5$ at $M_1 = 1 \text{ GeV}/c^2$ for three representative decay lengths.